

Coupled Model of Wave Damping, Quasilinear Heating, and Radial Transport Applied to Bumpy Tori

D. B. Batchelor, M. D. Carter, G. L. Chen, and C. L. Hedrick

Oak Ridge National Laboratory, Oak Ridge, Tennessee 37831

(Received 9 March 1987)

A simple Fokker-Planck model of rf heating is presented which includes quasilinear velocity diffusion, collisions, and particle transport by radial collisional diffusion and direct-drift losses. In addition, the influence of the incident-wave electric-field spatial profile on the velocity-space structure of the quasilinear operator and, in turn, the effect of the nonlinear distribution function on the wave field are included. Application is made to electron-cyclotron heating in the Elmo bumpy torus.

PACS numbers: 52.50.Gj, 52.25.Fi, 52.55.Hc

In the study of wave heating of plasmas, it is common to consider the wave propagation and damping, the velocity-space response of the plasma particles to the waves, and the transport of the deposited wave energy to be separable processes. Actually, however, these processes are coupled. We have developed a simple model that permits strong coupling among the spatial damping of the waves, the quasilinear evolution of the plasma distribution function, and the radial loss of plasma particles and energy. We have applied the model to an experiment in which the interaction of these processes is particularly strong, i.e., electron cyclotron heating of Elmo bumpy torus devices, EBT-I and EBT-S.¹ Our model gives good agreement with experimental results and shows that details of the spatial structure of the wave fields and the velocity-space structure of the quasilinear operator and loss processes can be quite significant.

The EBT devices consist of 24 toroidally linked simple mirrors that are heated by microwaves launched into each mirror at frequency $f_\mu = 18$ GHz in EBT-I and $f_\mu = 28$ GHz in EBT-S.¹ A fundamental cyclotron-resonance layer $\omega = 2\pi f_\mu = \Omega_{ce}$ (Ω_{ce} is the electron-cyclotron frequency) extends across the minor toroidal cross section about halfway between the midplane and each mirror throat. The dominant heating mechanism for the bulk plasma component is fundamental cyclotron absorption of extraordinary-mode power propagating from the high-field side which has been produced in the high-field region by multiple reflections and mode conversion of the ordinary mode.²

In mirror geometry, extraordinary-mode waves approaching fundamental resonance from the high-field side with wave number k_\parallel (magnetic beach configuration) are very strongly damped.^{3,4} Because the parallel velocity, v_\parallel , of the particles must satisfy the Doppler-shifted-resonance condition $v_\parallel = (\omega - \Omega_{ce})/k_\parallel$, the sharp decrease in wave amplitude near the resonance layer implies that particles having large v_\parallel are most strongly heated. In EBT devices the effective rotational transform that produces confinement against the vertical drift is provided by combined ∇B , $\mathbf{B} \times \nabla \phi$ (ϕ is ambipolar po-

tential), and curvature drifts in the poloidal direction. Since the sum of these drifts is velocity-space dependent, the loss rates of particles vary considerably with energy and pitch angle. At high energy ($\epsilon > e\phi$, where ϵ is particle energy), where $\mathbf{B} \times \nabla \phi$ drifts are dominated by magnetic drifts, passing particles and particles with pitch angle near the trapped-passing boundary are particularly lossy because the poloidal drift is small. Qualitatively, then, one expects the microwaves to couple to an energetic tail which is itself lossy and which is only weakly collisionally coupled to the bulk of the distribution.

We attempt to model the central region of EBT by solving a steady-state, bounce-averaged Fokker-Planck equation,

$$\nabla_v \cdot \Gamma_{rf} + \nabla_v \cdot \Gamma_{cc} = S(\mathbf{v}) - f/\tau(\mathbf{v}), \quad (1)$$

where Γ_{rf} is the velocity-space flux driven by the microwaves,⁵ Γ_{cc} is the flux driven by collisions,⁶ $S(\mathbf{v})$ is a particle source, and $\tau(\mathbf{v})$ is an effective lifetime that models radial-diffusion and direct-drift losses. A transformation of variables is made to (v, θ) , where v is particle speed and θ is pitch angle at the midplane. Computational details will be presented by Carter *et al.*⁷

The radial losses are treated by a zero-dimensional model in which each point of velocity space is assigned a loss rate $\tau(\mathbf{v})^{-1} = D(\mathbf{v})/(\Delta r)^2$, where $D(\mathbf{v})$ is a velocity-dependent radial-diffusion coefficient and Δr is a characteristic radius of the central plasma region. The diffusion coefficient is taken to be of the form $D = v_{90}(v)(\Delta x)^2$, where $v_{90}(v)$ is the energy-dependent 90° scattering frequency and Δx is the collisionally broadened neoclassical step size,

$$D(\mathbf{v}) = v_{90}(v)v_y^2(v, \theta)/[\Omega(v, \theta)^2 + v_{90}(v)^2], \quad (2)$$

where v_y is the bounce-averaged vertical-drift velocity and $\Omega(\mathbf{v})$ is the poloidal drift frequency as described by Spong and Hedrick.⁸ This diffusion coefficient, which takes into account radial drifts caused by toroidicity, is essentially the neoclassical particle-diffusion coefficient of Kovrizhnikh before being integrated over velocity

space.⁸

When the magnetic drift cancels the $\mathbf{B} \times \nabla \phi$ drift, the neoclassical step size becomes quite large and can exceed the size of the plasma. The diffusive model clearly breaks down, and losses occur by drifting directly out of the central region. Therefore, in regions of velocity space for which $\Delta x > \Delta r$ and the time to drift a distance Δr is less than the scattering time, the particle lifetime for direct loss is taken as $\tau = \Delta r / v_y$.

The microwave electric-field profile, $|E_-|$, is calculated by our assuming the plasma to be parallel stratified in the absorption layer near the fundamental cyclotron resonance.⁴ The warm-plasma dispersion relation is solved for complex k_{\parallel} by use of the numerically determined distribution function. When the distribution is Maxwellian, finite k_{\perp} makes a very small change in the $|E_-(s)|$ profile and, since the gyroradius is small at the temperatures of interest, the effect on the quasilinear operator can be neglected. With $k_{\perp} = 0$ the dispersion relation is of the form

$$\frac{c^2 k_{\parallel}^2}{\omega^2} = 1 + \frac{\omega_{pe}^2}{\omega k_{\parallel} v_e} \tilde{Z} \left(\frac{\omega - \Omega_{ce}}{k_{\parallel} v_e} \right), \quad (3)$$

where $\tilde{Z}(\zeta)$ is a generalized plasma dispersion function,

$$\tilde{Z}(\zeta) = \int_{-\infty}^{\infty} du_{\parallel} \frac{F(u_{\parallel})}{u_{\parallel} - \zeta}, \quad \text{Im} \zeta > 0,$$

$$F(u_{\parallel}) = \frac{v_e}{2\pi} \int_0^{\infty} dv_{\perp} v_{\perp} f(v_{\perp}, u_{\parallel} v_e).$$

Equation (3) is solved numerically for complex k_{\parallel} , and the profile of the right circular component of $|E_-|$ is obtained from $dP/ds = -2\text{Im}\{k_{\parallel}\}P(s)$, where $P(s) = c \text{Re}\{k_{\parallel}\} |E_-|^2 / (8\pi\omega)$ is the Poynting flux and s is distance along a field line from the $\omega = \Omega_{ce}$ location. This profile is evaluated at the Doppler-shifted-resonance location for each v, θ to obtain the quasilinear diffusion operator. The $|E_-|$ profile is initially calculated by our assuming the distribution to be Maxwellian. After solving Eq. (1) for f , we recalculate the $|E_-|$ profile from f and repeat the process to convergence.

In calculation of the collision operator in Eq. (1), the density (or temperature) of the Maxwellian background plasma is fixed. Then the temperature (or density) of the background is adjusted iteratively so that the collision operator in Eq. (1) provides zero net power. Thus, the power deposited in the test distribution by the quasilinear operator is balanced by diffusive and direct losses. At this point, the model is closed and contains six parameters: n , the electron density; P_{μ} , the microwave power; B_0 , the magnetic field at the midplane; M , the mirror ratio; $\nabla \phi$; and Δr . Of these parameters, all but Δr are machine parameters or can be estimated from experimental data. This leaves Δr as a free parameter which, since direct losses tend to dominate, scales τ approximately linearly. Our approach has been to choose a value of Δr to match the total energy-confinement time

given by a Monte Carlo transport simulation code⁶ for a specific set of plasma parameters. The value obtained, $\Delta r = 3$ cm, was fixed for all calculations discussed in this Letter. This value for Δr is not unexpected, because closed, nested contours of ambipolar potential exist only out to radii of 5 to 10 cm depending on the operating regime.⁶ Thus, the $\mathbf{B} \times \nabla \phi$ drift, which dominates confinement for lower energy particles, is directed away from the core outside the last closed potential contour ($r \gtrsim 5$ cm), and the value of Δr obtained by calibration with the Monte Carlo code is therefore reasonable.

In the experiment, a combination of diagnostics was used to determine the electron distribution function: Thomson scattering, which gives information primarily at low energies ($\epsilon < 200$ to 400 eV); soft-x-ray measurements, which give information in the 400-eV to 2-keV range; and a spectroscopic aluminum-impurity diagnostic, which gives a measure of average electron energy. We consider first a specific experimental case that was analyzed extensively by Swain *et al.*⁹ The plasma density is $n \approx 6 \times 10^{11} \text{ cm}^{-3}$, and the total microwave power at 28 GHz is $P_{\mu} = 150$ kW; this amounts to a power density of $\approx 3.4 \text{ W/cm}^2$ incident on each fundamental resonance surface. The ambipolar potential near the center was described by $\phi(r) = \phi_0 \{1 - [r/(15 \text{ cm})]^2\}$, where $\phi_0 \approx -400$ V. The bulk electron temperature from Thomson scattering was 78 eV, and in Ref. 9 the warm tail population was modeled as a 500-eV Maxwellian having density between 20% and 30% of the total. The total electron-energy confinement time for the central portion of the plasma τ_E was in the range 0.18 to 0.25 ms, and particle-confinement time τ_p , in the range 0.2 to 0.9 ms.

Figure 1 shows contours of the calculated distribution function for this case. Also shown are the pitch angles for which particles turn just at the cyclotron-resonance layer, the trapped-passing boundary, and the boundary of the region of direct particle loss. When the distribution function was integrated over θ , an "effective" temperature at different energies was determined from the slope. At low energy the temperature is ~ 104 eV, and at an energy of 2 keV the effective temperature is ~ 280 eV. The total energy-confinement time is $\tau_E = 0.18$ ms, and the particle-confinement time is $\tau_p = 0.54$ ms. These results are in quite reasonable agreement with the experimental estimates.

Since particles that turn before reaching the cyclotron resonance cannot be heated and the effect of the heating is to push particle turning points toward the resonance (Fig. 1), the cyclotron resonance acts as a stagnation layer. Therefore, the location in velocity space of the cyclotron resonance relative to the direct-loss boundary should influence heating and confinement. In particular, if the wave frequency is fixed, increasing the magnetic field moves the cyclotron resonance to a larger pitch angle and away from the lossy region of velocity space. Experiments were performed in EBT-I in which the

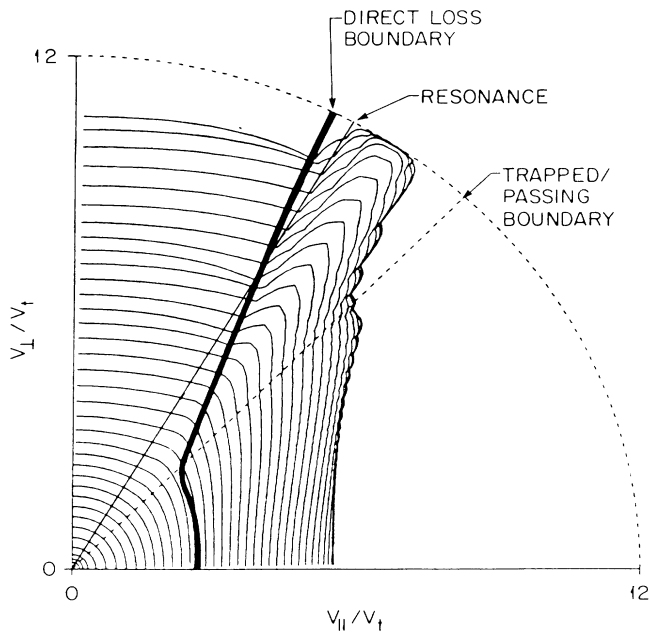


FIG. 1. Typical EBT distribution function with self-consistent power profile for $B=7.16$ kG, $n=6 \times 10^{11}$ cm $^{-3}$, and microwave power incident on each resonant surface equal to 3.4 W/cm 2 .

power was fixed and the magnetic field varied. An increase in line-average density was indeed observed with increasing field. Figure 2 shows measured average density and calculated density wherein the background temperature and wave-power density were held fixed. The close agreement should be taken only to indicate agreement in trend since in the experiment the hot-electroning location and other plasma parameters varied in response to the magnetic field.

In each of these calculations, the direct losses dominate the total confinement time. Taking moments of the loss terms in Eq. (1) with the distribution function in Fig. 1 shows that 83% of the power and 63% of the particles are directly lost. Increasing power draws out a more energetic tail and, since the tail resides in the region of large direct losses, this effect is increased. Experiments were conducted in which 20 kW of power was launched in the throat region of a single mirror cavity and directed on the fundamental cyclotron resonance, as well as 80 kW of power launched at the midplane of all cavities through the usual distribution system.¹⁰ In this case, the wave power density on resonance at the plasma center of the throat-launch cavity was approximately six times that for normal operation at 100 kW total power. The experimental result was that a very strong tail population developed in the throat-launch cavity. The plasma density dropped, and measurements in cavities opposite the throat-launch cavity showed no increase in the bulk plasma temperature. In addition, thermocouples in the wall of the throat-launch cavity showed a large increase in

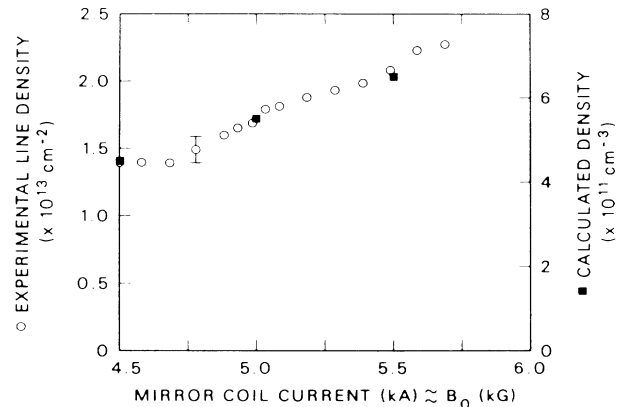


FIG. 2. Experimentally measured line density and calculated equilibrium density. Both increase with increasing magnetic field (calculations for $T_e = T_i = 100$ eV).

power deposited in the region where open drift surfaces intersect the wall. Figure 3 shows calculated values of τ_E , τ_p , and average particle energy versus $\langle E \rangle$ incident wave power density. The parameters are the same as those for Fig. 1 except that $n=9 \times 10^{11}$ cm $^{-3}$. The power range shown is approximately that for the experiment. One sees that the average particle-energy increase is accounted for mostly by an increase in the tail population because the increase in bulk temperature is only $\sim 40\%$. However, this increased energy is rapidly lost, direct losses at the highest power accounting for 92% of the total.

This closed model has given good agreement with a variety of experimental observations in EBT-I and EBT-S. This agreement was obtained without adjustment of

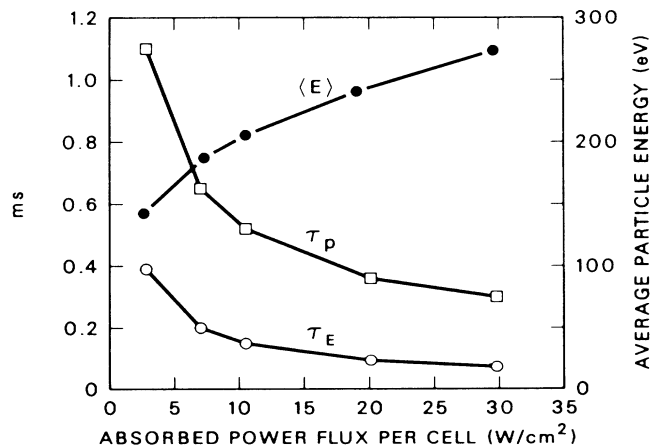


FIG. 3. Confinement times making a transition from diffusively dominated transport at low powers to direct-loss-dominated transport at higher powers for standard EBT parameters ($B_0=7.16$ kG, $\omega=28$ GHz, $n=9 \times 10^{11}$ cm $^{-3}$, and $\phi=400$ V). Average particle energy indicates distortion of the distribution function.

the free parameter of the model (Δr); only the experimental input parameters ($n, B_0, P_\mu, f_\mu, \phi$) were changed. In particular, the model indicates that simple neoclassical confinement associated with a small perturbation of a Maxwellian distribution is not to be expected in EBT devices, even if any anomalous transport associated with instabilities is neglected. The large direct losses are associated with the proximity of the heating stagnation zone to the lossy region of velocity space and the decidedly non-Maxwellian nature of the energetic population. This problem has been addressed in the proposed Elmo bumpy square device,¹¹ in which the heating zone is well separated from a much smaller lossy region of velocity space. Similar calculations for Elmo bumpy square do show greatly improved confinement.⁷

For this toroidal device the simple 0D model for radial transport and 1D model for the wave-field profile succeed because losses are dominated by single-particle orbits with large radial excursions and damping occurs in a thin layer due to parallel stratification of $|B|$. This is to be compared to models of electron cyclotron heating (ECH) in open mirrors¹² in which end losses can also be treated in zero spatial dimensions but the waves propagate perpendicular to \mathbf{B} . There the wave-field profile (hence velocity-space diffusion) is determined more by antenna placement than by details of wave damping on the self-consistent distribution function.

Of much more general interest than the application to bumpy tori is the indication given by this model that the details of coupling among the different physical processes involved are important. For example if a constant $|E - |$ profile is used rather than the self-consistent one, the quasilinear operator couples up to 2 orders of magnitude more power to the distribution function than is actually

carried by the wave. The method used here to treat radial transport is probably not useful for diffusive losses in larger devices with better confinement. However, it may well be applicable to prompt losses, such as ripple-trapped particles in tokamaks or helically trapped particles in stellarators that are strongly driven by ion cyclotron-resonance heating.

This research was sponsored by the Office of Fusion Energy, U. S. Department of Energy, under Contract No. DE-AC05-84OR21400 with Martin Marietta Energy Systems, Inc.

¹R. J. Colchin *et al.*, *Plasma Phys.* **25**, 1228 (1983).

²D. B. Batchelor, R. C. Goldfinger, and D. A. Rasmussen, *Phys. Fluids* **27**, 948 (1984).

³T. H. Stix, *The Theory of Plasma Waves* (McGraw-Hill, New York, 1960).

⁴A. Fruchtman, K. Riedel, H. Weitzner, and D. B. Batchelor, *Phys. Fluids* **30**, 115 (1987).

⁵I. B. Bernstein and D. C. Baxter, *Phys. Fluids* **24**, 108 (1981).

⁶J. S. Tolliver, *Phys. Fluids* **28**, 1083 (1985).

⁷M. D. Carter, D. B. Batchelor, C. L. Hedrick, and G. L. Chen (to be published).

⁸D. A. Spong and C. L. Hedrick, *Phys. Fluids* **23**, 1903 (1980).

⁹D. W. Swain, J. A. Cobble, D. L. Hillis, R. K. Richards, and T. Uekan, *Phys. Fluids* **28**, 1922 (1985).

¹⁰D. A. Rasmussen *et al.*, *Phys. Fluids* **29**, 318 (1986).

¹¹R. A. Dory *et al.*, Oak Ridge National Laboratory Report No. ORNL/TM-9994, 1986 (unpublished).

¹²Y. Matsuda and T. D. Rognlien, *Phys. Fluids* **26**, 2778 (1983).